Qianli Ma, Liheng Chen*, Ruibin Wang, Rendang Yang and J.Y. Zhu*

Direct production of lignin nanoparticles (LNPs) from wood using *p*-toluenesulfonic acid in an aqueous system at 80°C: characterization of LNP morphology, size, and surface charge

https://doi.org/10.1515/hf-2018-0033
Received February 13, 2018; accepted June 4, 2018; previously published online June 30, 2018

Abstract: Lignin nanoparticles (LNPs) from renewable lignocelluloses can be a valuable building block for a variety of applications and could contribute to the economic development in rural agricultural communities. Current technologies for producing LNPs are not cost effective and use toxic solvents. In this study, LNPs were produced by fractionating poplar wood at ≤80°C with a recyclable hydrotrope *p*-toluenesulfonic acid (*p*-TsOH) in an aqueous system. The dissolved lignin was separated as LNPs simply by diluting the spent liquor (SL) to the minimal hydrotrope concentration (HC_{min}) of 11.5%. The *p*-TsOH, a solid acid, can be easily recycled by re-concentrating the diluted SL after lignin separation. The LNP size, morphology, and surface charge were controlled by the dilution ratio, speed, pH, and ionic strength of the LNP sol. The LNPs were analyzed by dynamic light scattering (DLS) and found to be fairly stable in terms of mean particle size and surface charge over a period of 2 weeks. Fractionation conditions also affected LNP properties.

Keywords: hydrotrope, lignin nanoparticles (LNPs), low temperature fractionation, particle size and morphology, particle surface charge and aggregation

Introduction

Native lignins are abundant renewable polyaromatic polymers composed of phenylpropanoid units, which have a high potential for a variety of applications, but cannot be easily isolated from lignocellulosic materials (Ragauskas et al. 2014). On the other hand, technical lignins produced in the course of the chemical pulping of lignocelluloses, are commercially available in large quantities. These are usually burned in pulp mill boilers for the recovery of pulping chemicals. Lignosulfonates from acidic sulfite pulping can be used immediately as dispersants, however, the valorization of lignins from kraft pulping is very limited. It would be rewarding to develop further lignin utilization techniques (Li et al. 2015; Wang et al. 2015; Shuai et al. 2016; Tupciauskas et al. 2017).

Lignin nanoparticles (LNPs) attracted great interest recently because of their large surface area, which can be used as anti-oxidants, ultraviolet (UV) light absorbing and hydrophobic materials, which are also biodegradable (Lu et al. 2012; Richter et al. 2015). LNPs can also be integrated as co-polymer in rubber (Jiang et al. 2013) and other composites (Nair et al. 2014), surfactants in pickering emulsion (Qian et al. 2014; Ago et al. 2016), and as vehicles for drug delivery (Tortora et al. 2014). LNPs can be obtained by the dissolving of commercial technical lignins through chemical reactions (Popa et al. 2011; Cheng et al. 2012), or by means of solvents such as ethylene glycol (Frangville et al. 2012), acetone (Richter et al. 2016), tetrahydrofuran (THF) (Lievonen et al. 2016), or N,N-dimethylformamide (DMF) (Qian et al. 2014; Ago et al. 2016; Myint et al. 2016), with subsequent acid precipitation (Popa et al. 2011; Frangville et al. 2012; Richter et al. 2016) or hexane (Qian et al. 2014), dialysis (Lievonen et al. 2016), atomization and drying (Ago et al. 2016), or antisolvent particle formation (Lu et al. 2012; Myint et al. 2016). The sustainable commercial implementation of these processes is difficult because of environmental concerns and high costs of solvents and their recovery. The application of chemically modified lignins is limited for many purposes. Mechanical treatments such as ultrasonication (Tortora et al. 2014) and mechanical milling (Shikinaka et al. 2010; Nair et al. 2014) have been applied to produce LNPs from lignocellulosic materials, but these approaches are energy intensive.

It has been demonstrated by Chen et al. (2017) that the hydrotropic *p*-toluenesulfonic acid (*p*-TsOH) is well-suited to achieve near-complete solubilization of wood lignin in an aqueous solution during 20 min at ≤80°C.

***Corresponding authors: Liheng Chen,** Key Laboratory of Biomaterials of Guangdong Higher Education Institute, Department of Biomedical Engineering, Jinan University, Guangzhou, China, e-mail: lihengchen@jnu.edu.cn; and **J.Y. Zhu,** USDA Forest Service, Forest Products Laboratory, Madison, WI, USA, Phone: +1-608 231 9520, e-mail: jzhu@fs.fed.us
Qianli Ma and Ruibin Wang: State Key Laboratory of Pulp and Paper Engineering, South China University of Technology, Guangzhou, China; and USDA Forest Service, Forest Products Laboratory, Madison, WI, USA
Rendang Yang: State Key Laboratory of Pulp and Paper Engineering, South China University of Technology, Guangzhou, China

The key advantage of hydrotrope chemistry (Shimizu and Matubayasi 2014; Kunz et al. 2016) is that the dissolution of hydrophobic materials such as lignin is accomplished in an aqueous system, i.e. the handling of toxic and costly organic solvents can be avoided. The dissolved lignin can be precipitated in the form of LNPs simply by dilution with water to below the *p*-TsOH minimal hydrotrope concentration (HC_{min}), which is ca. 11.5% (Bian et al. 2017; Chen et al. 2017). Lignin precipitation facilitates the efficient recycling and reuse of *p*-TsOH. Furthermore, *p*-TsOH in hydrotrope chemistry at temperatures below the water boiling point resulted in LNPs in a relatively native state. Compared with other LNP production processes, *p*-TsOH fractionation has substantial advantages in terms of chemical recovery, environmental impact, and LNP properties.

In the present study, the control of the properties of LNPs resulting from *p*-TsOH fractionation is reported, and the focus is on the precipitation conditions (dilution ratio, speed, and solution pH and ionic strength) in terms of LNP morphology, particle size, and surface charge, which are critical to many applications (Kumari et al. 2010). The goal is to obtain tailored products via the economic and environmentally benign and sustainable production of LNPs.

Materials and methods

Poplar wood, *Populus deltoides* Bartr. *ex* Marsh × *P. nigra* L., harvested from Hugo Sauer Nursery in Rhinelander, WI, USA, was the raw material for wood powder preparation via Wiley milling and sieving through 20-mesh sieve.

Lignin removal: *p*-Toluenesulfonic acid (*p*-TsOH) of ACS reagent grade was obtained from Sigma-Aldrich (St. Louis, MO, USA). Concentrated aqueous *p*-TsOH solutions with concentration between 70 and 85% were prepared in multiple-neck flasks by solubilizing *p*-TsOH in deionized (DI) water. Each flask was heated to 65–80°C in a glycerol bath (heating plate, magnetic stirring) according to Chen et al. (2017). Ten grams (o.d. weight) of wood powder with ca. 35% moisture content were added to 100 ml *p*-TsOH and heated as shown schematically in Figure 1a. At the end of fractionation, ca. 80 ml DI water was added to stop the reaction, in the course of which the *p*-TsOH concentration was diluted to 40%. The resultant spent liquor (SL) was filtrated over filter paper under vacuum to separate the water-insoluble solids (WIS). The filtrate was diluted to 10% with DI water and then centrifuged at 3000 *g* for 10 min. Two fractions of lignin particles were obtained, one in the supernatant and another in the precipitated solids. The precipitated lignin can be resuspended in DI water for further analyses or utilization.

LNP size, morphology, and surface charge were characterized using atomic force microscopy (AFM Workshop, Signal Hill, CA, USA) and dynamic light scattering (DLS) analysis (Nanobrook Omni, Brookhaven Instruments, Holtsville, NY, USA). The suspensions were sonicated for ca. 5 min. A drop of the suspension was dispersed on a mica substrate. After air-drying at ambient temperature, AFM images were taken in vibrating tapping mode at 160–225 kHz by means of a silicon cantilever having a tip curvature radius of 10–15 nm. The height distributions of LNPs from the AFM-measured topography of the sample were analyzed using Gwyddion software installed on the AFM system (Department of Nanometrology, Czech Metrology Institute, Czech Republic, 64-bit). During LNP particle size analysis via DLS, each sample was circulated five times for a total of 10 min to obtain average size and mean zeta potentials.

Results and discussion

Verification of colloidal lignin particle sol system

Hydrotrope chemistry often works best with hardwoods (Procter 1971) such as poplar, which can be grown on marginal land (Lazarus et al. 2015). In this study, the SL from the dissolved poplar wood – designated as $P_{75Tol,\ 80T,\ 20\ min}$, meaning *p*-TsOH concentration of 75%, 80°C, and 20 min reaction time – was diluted to 10% [below the HC_{min} of *p*-TsOH of 11.5% (Chen et al. 2017)]. Ten milliliters of the diluted liquor was centrifuged at 3000 *g* for 10 min to precipitate the dissolved lignin (Figure 1b, left tube) and further diluted to *p*-TsOH concentration of ca. 2% by removing 7.5 ml of the supernatant and adding 10 ml DI water to the tube. Almost all dissolved lignin was precipitated through centrifugation, as was visible on the clear supernatant of the SL (Figure 1b, middle tube). The mechanism is that the high ionic strength compresses the double electric layer on the surface of suspended lignin particles leading to aggregate formation of the lignin particles, which precipitate under the centrifugation force. After removing most of the ions through further centrifugation and removal of supernatant, a suspension is obtained with a *p*-TsOH concentration of 0.4%, in which the charged particles cannot be precipitated via centrifugation at 3000 *g* for 10 min, because of the strong electrostatic repulsions among them. Therefore, the supernatant is turbid (Figure 1b, the right tube) with a significant Tyndall effect; that is, the red laser beam was highly visible in the direction perpendicular to its incident direction due to light scattering of very small particles (Figure 1c). Accordingly, the dispersion is an aqueous sol, or a colloidal system that contains LNPs.

Effect of fractionation conditions on LNP properties

More severe reaction conditions, for example, with more than 70% wood lignin dissolution, resulted in a larger mean LNP size measured by DLS (Table 1). The amount of dissolved lignin correlated well with LNP size (Figure 2). Higher

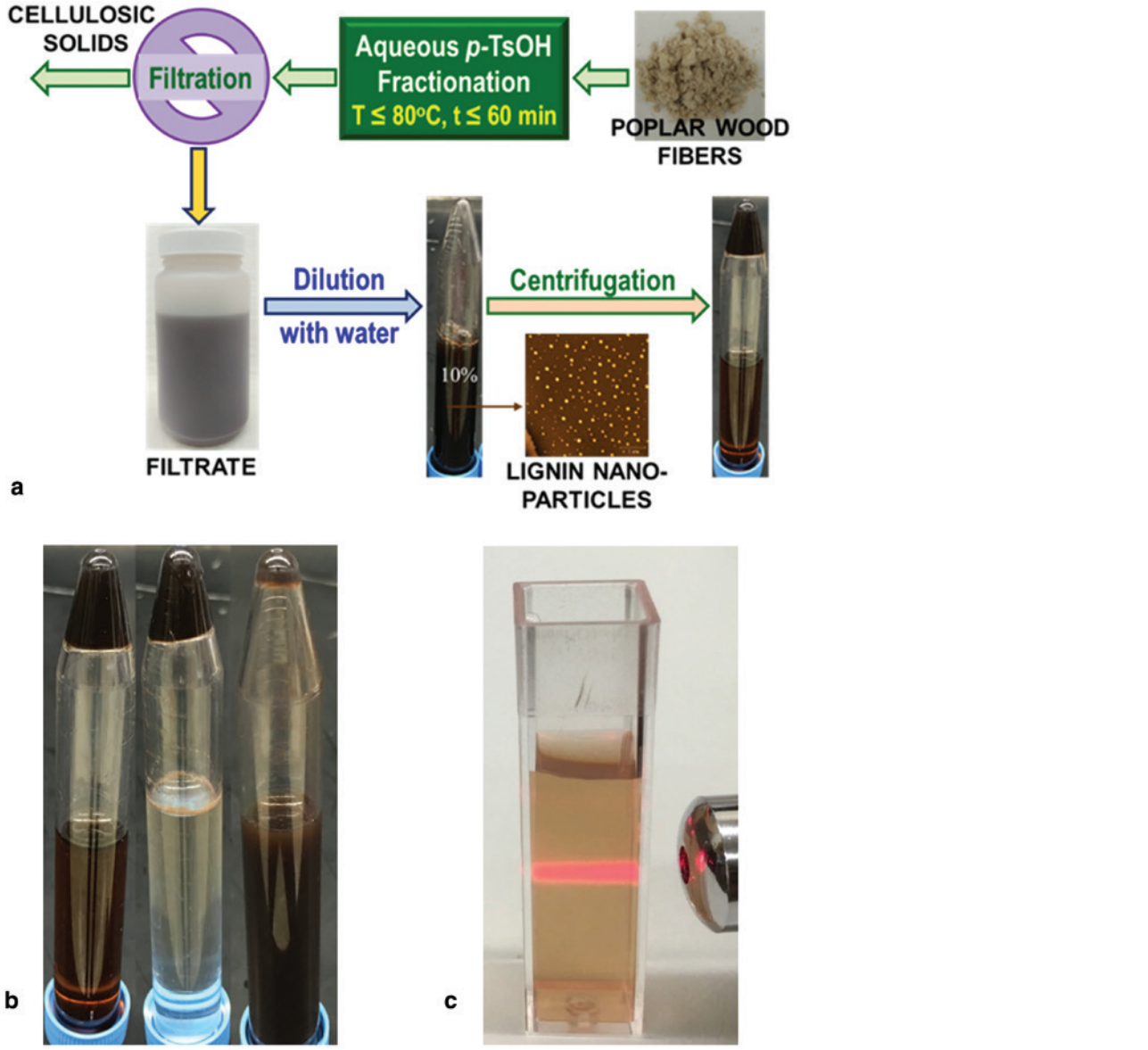

Figure 1: Graphical description of experiments carried out in this study.
(a) A schematic flow diagram showing *p*-TsOH fractionation of wood to produce lignin nanoparticles in an aqueous system at T ≤ 80°C for <60 min. (b) Images of diluted and centrifuged aqueous *p*-TsOH spent liquor showing precipitation of lignin (left and middle tubes), and turbid lignin particle suspension (right tube). (c) Laser light scattering of the turbid lignin particle suspension in b (right tube) showing the Tyndall effect.

lignin dissolution leads to a higher LNP concentration in the diluted SL than in a fractionation run with lower lignin dissolution, when both SLs of *p*-TsOH were diluted to 10%. A higher lignin concentration increases particle aggregation simply due to the higher collision probability among lignin particles. Under more severe conditions, more lignin with a higher molecular weight is solubilized than would occur under milder conditions (Bian et al. 2017; Chen et al. 2017), which can also affect LNP aggregation. The data concerning dissolved lignin in Table 1 show the lignin percentages in the unfractionated poplar wood. The dissolved lignin in SL was determined from the lignin mass balance by evaluating the residual lignin in the washed WIS. For verification, the gravimetrical lignin determination was carried out directly from the precipitated dissolved lignin after diluting the SL to 2% followed by washing. Discrepancies between the results of these methods (Table 1) are due to precipitation losses by the washing of dissolved lignin.

Nuclear magnetic resonance (NMR) analyses indicated (Chen et al. 2017) that the dissolved lignin does not contain carbohydrates. Furthermore, *p*-TsOH fractionation had a good selectivity in solubilizing lignin and

Table 1: Lignin nanoparticles from different fractionations of poplar wood measured from the spent *p*-TsOH acid liquor rapidly diluted to 10% and then dialyzed to pH 4.5.

Treatment codes	Lignin dissolved (%)		Diam.	Zeta pot.
	Solid	Liquor	(nm)	(mV)
$P_{70Tol, 50T, 20\ min}$	29.8	25.0	345±2	−40.0±0.2
$P_{70Tol, 65T, 20\ min}$	65.1	63.9	372±8	−36.5±0.2
$P_{70Tol, 65T, 35\ min}$	63.9	60.3	414±2	−41.4±1.0
$P_{70Tol, 80T, 20\ min}$	77.6	68.2	442±4	−35.1±0.3
$P_{75Tol, 65T, 20\ min}$	71.6	63.9	439±5	−33.8±0.7
$P_{75Tol, 65T, 35\ min}$	77.4	60.7	475±3	−41.1±1.2
$P_{75Tol, 65T, 60\ min}$	81.0	58.7	500±2	−36.7±2.2
$P_{75Tol, 80T, 20\ min}$	85.5	73.7	467±3	−37.9±3.6
$P_{80Tol, 80T, 20\ min}$	90.7	78.6	530±7	−34.1±1.3

hemicelluloses, but not cellulose. As shown in Table 2, most of the fractionation runs retained over 90% of the cellulose in WIS, while solubilizing 70–90% of the lignin, and over 75% and 50% of the xylan and mannan, respectively. The washed WIS can be submitted to enzymatic hydrolysis and the resulting sugar yields will be excellent (Chen et al. 2017). The WIS is also suitable for producing lignin-containing (hydrophobic) cellulose nanofibrils via subsequent mechanical fibrillation with low energy input (Bian et al. 2017). The solubilized sugars in the SL were found to be mainly xylose (Table 2). The solubilized sugars can be converted into furans as valuable chemicals with *p*-TsOH without additional chemicals (Ji et al. 2016). *p*-TsOH can then be reused or recovered after the separation of furans through evaporation.

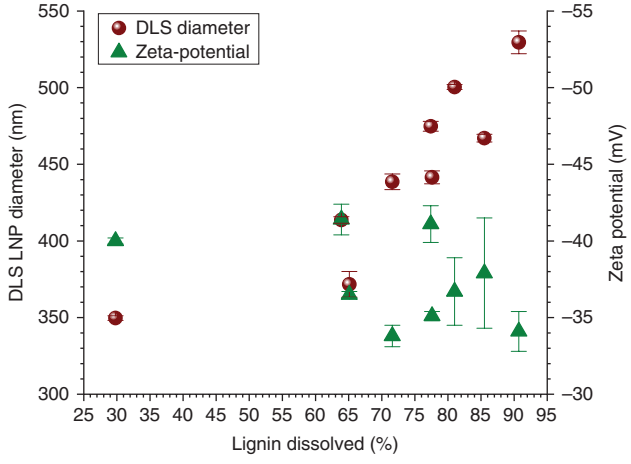

Figure 2: Correlation between DLS measured lignin particle size and the amount of lignin dissolved through *p*-TsOH fractionation of poplar at different severities.
The DLS size was measured from the diluted *p*-TsOH spent liquors at 10 wt% then dialyzed to pH 4.5.

Effects of spent liquor dilution and speed of dilution on LNP size and morphology

Five grams of *p*-TsOH SL (40% conc.) from the run $P_{75Tol, 80T, 20\ min}$ was mixed with 15 g DI water to 10% by a peristaltic pump at four flow rates of 0.19, 0.95, 2.85, and 5.71 ml min^{-1}. As the final dilution factors were uniformly 400%, the rates of dilution were expressed in min during the dilution period. The fastest dilution rate was achieved by manually adding 15 g of water into the flask in 1 s (0.0167 min). The dissolved lignin aggregated, when the SL was diluted to 10% (below the HC_{min} of 11.5%). DLS measurements indicated that reducing the rate of dilution increased LNP size (Figure 3a). The DLS-measured particle sizes were also qualitatively in agreement with the lateral diameters taken from AFM images (Figure 3b–d). The particle size increment is a direct result of dissolved lignin aggregation (Chen et al. 2017). Apparently, a slow dilution increased the aggregation time and larger particle sizes were seen as a result of fast dilution. A longer aggregation time also led to thicker lignin aggregates, as confirmed by the AFM height distribution measurements (Figure 3e). The LNP sample from very fast dilution, however, had a fairly narrow height distribution with a mean height of ≈15 nm. Deduced from AFM measurements, LNPs are oblate type spheroid nanoparticles and have an average aspect ratio (lateral diameter over height) of ≈10.

If the *p*-TsOH liquor concentration from 40% was diluted, the LNP size increased with the extent of dilution as shown in Figure 4a. Similarly, AFM measurements qualitatively verified the lateral size and thickness size increment of the LNPs (Figure 4b–e), respectively.

Effects of pH and ionic strength on lignin aggregation

The SL from $P_{75Tol, 80T, 20\ min}$ was quickly diluted from 40% to 10% and then dialyzed and the terminal pH was ≈4.5. The average zeta potential of the LNPs in the dialyzed sample was around −35 mV (Figure 2). Centrifugation removes larger particles in a suspension, i.e. centrifugation fractionates LNPs according to size as demonstrated by Bian et al. (2017) and Chen et al. (2017). The smaller particles are bearing greater charges, i.e. around −45 mV for LNPs <280 nm (Figure 5).

To investigate the effects of pH, NaOH, or HCl, solution at 0.1 mol l^{-1} were added to the supernatants after centrifugation. The LNP particle sizes were relatively stable between pH 3 and 10, while a slight size reduction was seen at pH 7.5 followed by a slight size increment at pH 10 (Figure 6a). Reducing pH below 3 or increasing pH above 10 resulted in

Table 2: Chemical compositions of *p*-TsOH fractionated poplar NE222 samples under different treatment conditions.

	Water-insoluble solids (WIS)					Spent liquor				
Sample label[a]	Solids yield (%)	Glucan (%)	Xylan (%)	Mannan (%)	Lignin (%)	Glc (gl^{-1})	Xyl (gl^{-1})	Man (gl^{-1})	AA (gl^{-1})	FAL[b] (gl^{-1})
Untr. NE222	100	45.7	14.9	4.6	23.4					
$P_{70Tot, 50T, 20\ min}$	78.9	56.8	8.8	3.3	20.6					
		(97.9)	(46.7)	(56.4)	(69.4)					
$P_{70Tot, 65T, 20\ min}$	68.4	61.6	6.5	4.3	11.8					
		(92.2)	(29.8)	(63.9)	(34.4)					
$P_{70Tot, 65T, 35\ min}$	64.1	68.0	6.6	4.6	13.0	1.3	10.1	1.5	1.5	0.0
		(95.3)	(28.4)	(64.0)	(35.7)	(2.5)	(59.5)	(29.9)		(0.7)
$P_{70Tot, 80T, 20\ min}$	58.9	63.0	6.5	4.3	8.8	1.5	11.0	1.8	1.6	0.13
		(81.1)	(24.5)	(53.8)	(22.1)	(3.0)	(65.0)	(35.2)		(1.2)
$P_{75Tot, 65T, 20\ min}$	60.7	71.8	5.8	4.9	10.8	1.4	10.8	1.7	1.5	0.10
		(95.4)	(23.8)	(63.7)	(28.0)	(2.7)	(64.0)	(32.4)		(0.9)
$P_{75Tol, 65T, 35\ min}$	59.0	71.7	6.0	4.0	8.9	1.3	10.3	1.7	1.4	0.10
		(94.5)	(23.9)	(51.3)	(22.3)	(2.6)	(60.8)	(32.4)		(0.9)
$P_{75Tot, 65T, 60\ min}$	57.0	74.7	5.0	4.3	7.4	1.7	10.7	1.8	1.5	0.14
		(93.1)	(19.2)	(52.8)	(17.9)	(3.2)	(63.4)	(34.6)		(1.2)
$P_{75Tot, 80T, 20\ min}$	55.0	72.4	5.2	4.4	6.1	1.8	10.9	2.0	1.5	0.19
		(87.1)	(19.1)	(52.7)	(14.4)	(3.6)	(64.2)	(39.7)		(1.7)
$P_{80Tot, 80T, 20\ min}$	51.9	72.3	3.7	3.7	4.2	2.3	9.9	2.2	1.4	0.33
		(81.9)	(13.0)	(41.8)	(9.2)	(4.6)	(58.4)	(43.9)		(3.1)

[a]($P_{xxTot, yyT, zz\ min}$) stands for *p*-TsOH concentration in wt%, reaction temperature in °C and reaction duration in min.
[b]Yields are based on xylan content in NE222. 5-hydroxymethylfurfural (HMF) in spent liquors were not detectable.
The numbers in the parentheses are component yields based on component in the untreated NE222 (data from Chen et al., *Sci. Adv.* 2017;3: e1701735). AA, Acetic acid; FAL, furfural.

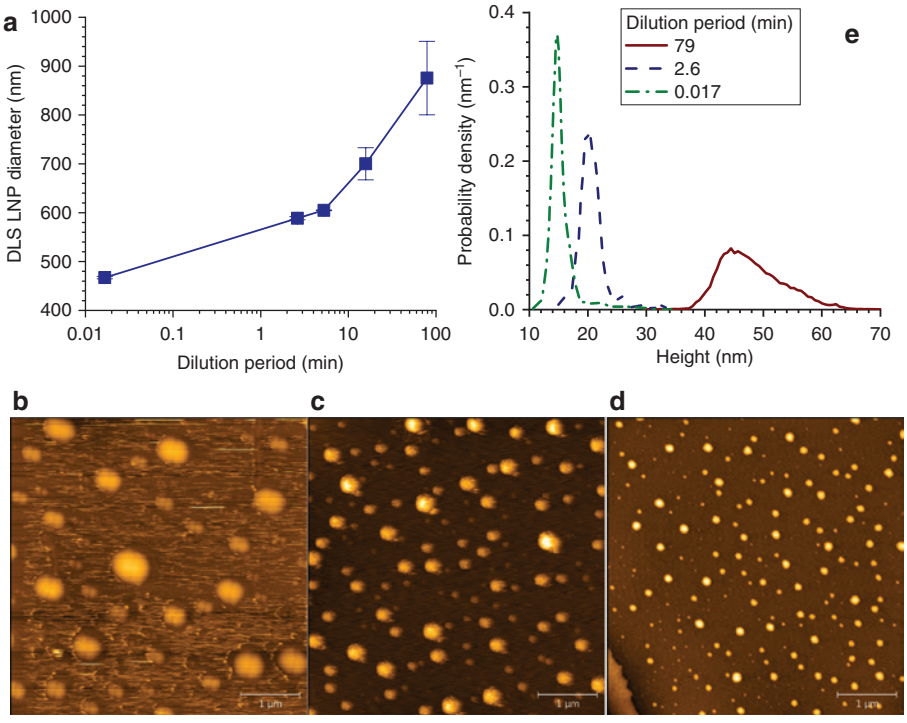

Figure 3: Effect of speed in diluting spent *p*-TsOH liquor (from 40% to 10%) on the resultant LNP size and morphology.
(a) Dynamic light scattering (DLS) measured LNP size; (b–d) AFM images of LNP at dilution period of 79 (b), 2.6 (c), and 0.0167 (d) min, respectively; (e) AFM measured LNP height distributions for the LNPs shown in b–d.

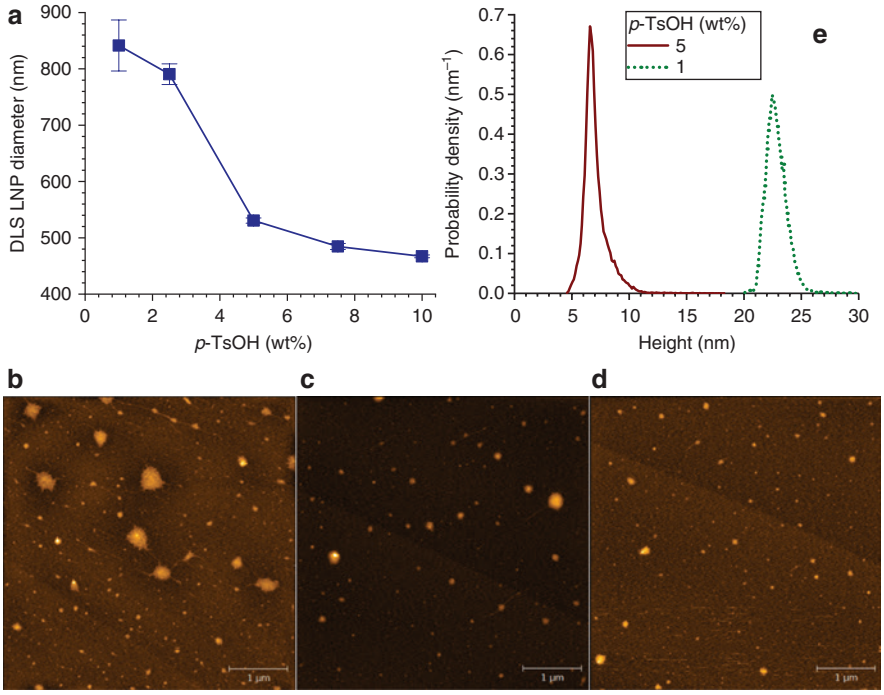

Figure 4: Effect of the extent of spent *p*-TsOH liquor dilution on the resultant LNP size and morphology.
(a) Dynamic light scattering (DLS) measured LNP size; (b–d) AFM images of LNP at *p*-TsOH concentration of 1 (b), 2 (c), and 5 (d) %, respectively; (e) AFM measured LNP height distributions for the LNP shown in b and d.

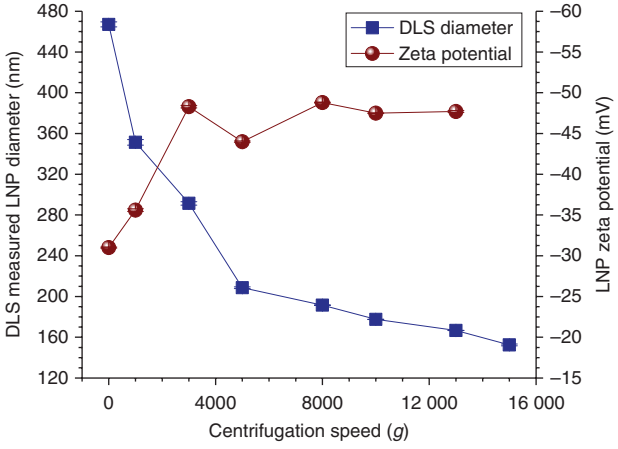

Figure 5: Fractionating lignin nanoparticles by size through centrifugation.
The reported DLS sizes were measured in the supernatants after centrifugation at the reported speeds. The initial lignin particle suspension sample was from P75T80t20 after diluting the spent *p*-TsOH liquor to 10 wt% and then dialyzed to pH 4.5.

a rapid increase in LNP size. This was also verified by AFM imaging (Figure 6b–e). The results in Figure 6a indicate that pH is a good parameter to control LNP size.

With increasing pH, the LNP zeta potential (ZP) decreased rapidly from about –4 mV to ≈ –50 mV at pH 7.5 and then increased rapidly at pH 12. The ZP_{peak} corresponded closely to the smallest LNP size (Figure 6a), i.e. the electrostatic repulsion plays a major role in particle aggregation. The relatively stable LNP size in the pH range between 3 and 10 is a result of high surface charge (Figure 6a). A ZP of –25 mV or lower is required to avoid substantial lignin particle aggregation, as visible on the rapid LNP increment of ZP above –25 mV.

The effect of ionic strength on LNP size was evaluated by spiking NaCl solution into a dialyzed LNP suspension of pH 6.4. With increasing NaCl concentration towards 20 mM, the ZP of the LNP increased from –50 mV to –25 mV and at that point there was a rapid increase in particle size due to aggregations (Figure 7a). This critical ZP of –25 mV is in agreement with the pH results (Figure 7a). The AFM imaging (Figure 7b–d) and AFM-height distributions (Figure 7e) clearly demonstrate the aggregation.

Stability of LNP particle size

Colloidal stability of LNPs is important in practice. The diluted *p*-TsOH SL from $P75_{Tol,\ 80T,\ 20\ min}$ at 10% concentration after dialyzing to pH ≈ 4.5 was checked again and centrifuged at 3000 *g* for 10 min. The precipitated lignin was re-suspended in DI water. Vigorous hand shaking was applied before DLS analyses. The LNP size in the

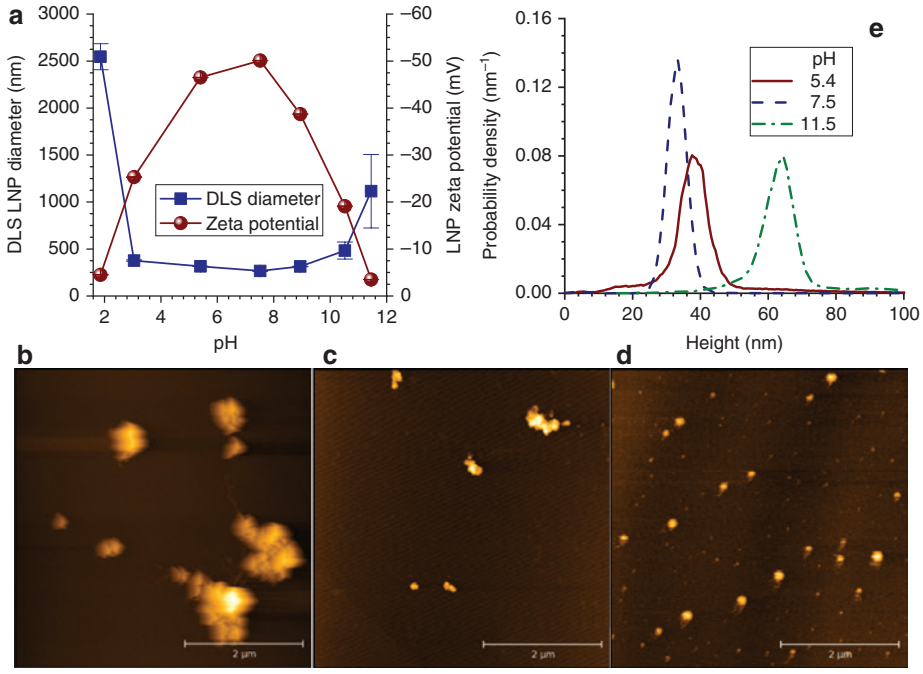

Figure 6: Effect of pH on the resultant LNP size and morphology in a supernatant from centrifuging a dialyzed LNP suspension (pH 4.5) at 3000 *g* for 10 min.
(a) Dynamic light scattering (DLS) measured LNP size; (b–d) AFM images of LNP at pH 11.5 (b), 7.5 (c), and 5.4 (d), respectively; (e) AFM measured LNP height distributions for the LNP shown in b–d.

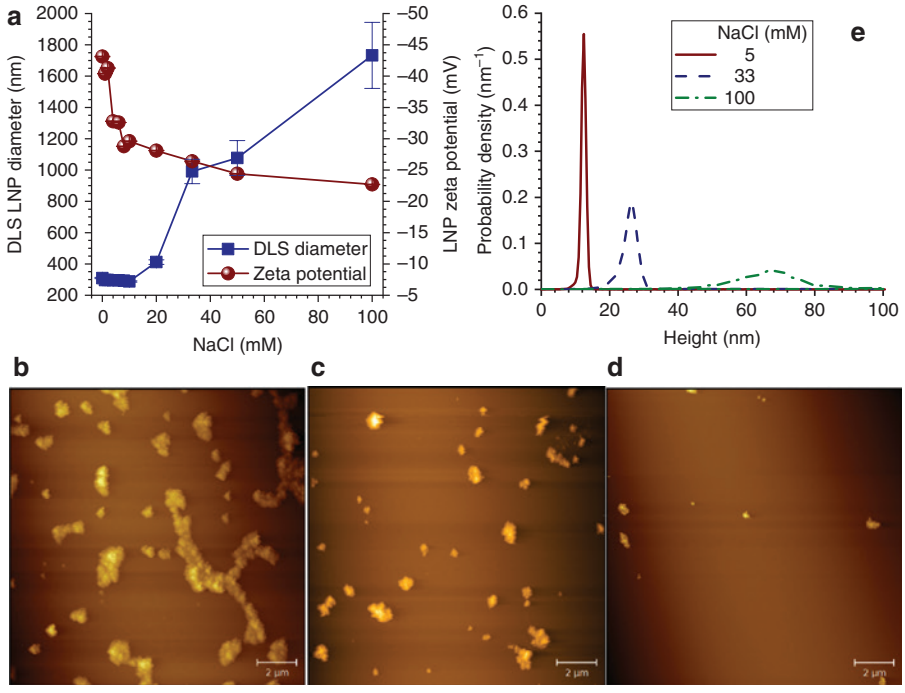

Figure 7: Effect of ionic strength on the resultant LNP size and morphology in a supernatant after centrifugation of a dialyzed LNP suspension (pH 4.5) at 3000 *g* for 10 min.
(a) Dynamic light scattering (DLS) measured LNP size; (b–d) AFM images of LNP at NaCl concentration in mM of 100 (b), 33 (c), and 5 (d), respectively; (e) AFM measured LNP height distributions for the LNP shown in b–d.

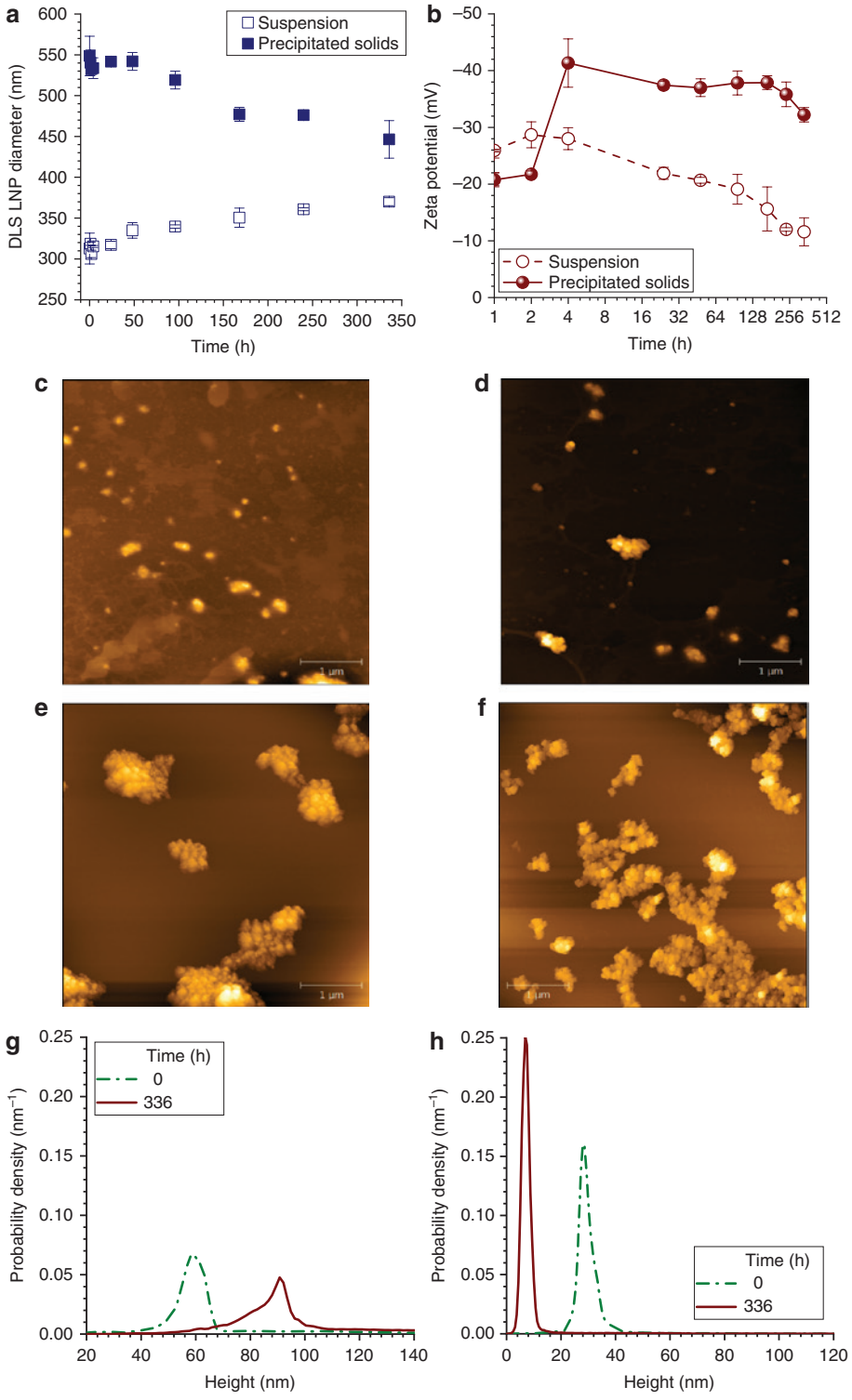

Figure 8: LNP particle size stability.
(a and b) Effects of storage time on DLS measured the size (a) and zeta potential (b); (c–f) AFM images of LNPs at the beginning of storage in the supernatant (c) and in the suspension of the resuspended solids (d), and at the end of storage in the supernatant (e) and in the suspension of the resuspended solids (f); (g and h) AFM measured height distributions of LNPs in the supernatant (g) and in the suspension of the resuspended solids (h).

supernatant increased gradually during a period of 2 weeks from ca. 310 to 370 nm (Figure 8a), while the mean ZP gradually increased from –28 mV to –11 mV (Figure 8b). AFM images obtained before and after 2 weeks confirmed the LNP size increment due to aggregation (Figure 8c and d). The particle thickness was also elevated, as shown by the AFM measurements (Figure 8g). Obviously, a long storage time reduced the stability of colloidal particles.

The particle sizes of the re-suspended precipitated lignin decreased over a period of 2 weeks from 540 nm to 450 nm (Figure 8a). At time zero, these particles were larger than those from LNPs in the supernatant from centrifuging as clearly seen by AFM imaging (Figure 8c vs. 8e), and showed precipitation tendencies as manifested in biased sampling of more un-precipitated smaller particles despite hand-shaking before DLS analyses. According to results in Figure 6b, the resuspension of the precipitated particles increased the pH of the suspension, which resulted in a high surface charge (Figure 8b), and prevented aggregations during drying for AFM imaging (Figure 8f). The AFM thickness measurements (Figure 8g and h) are in agreement with the DLS data.

Conclusions

This study demonstrates a facile and sustainable procedure for producing LNPs directly from wood at ≤80°C based on the *p*-TsOH approaoch. *p*-TsOH is an easily recyclable hydrotropic acid, which dissolves wood lignin and the lignin can be precipitated by dilution to the HC_{min}. Dilution speed and ratio, fractionation conditions, pH, and ionic strength of the LNP sol are the parameters used to control the resultant LNP size, morphology, and surface charge. A stability study over a 2-week period showed by dialyzing the LNP sol that the LNP size and surface charge are fairly stable.

Acknowledgments: This work was partially supported by the U.S. Forest Service, the 111 plan and Guangdong Provincial Science & Technology Plan Projects (No. 2015B020241001), the State Key Laboratory of Pulp and Paper Engineering (No. 2015ZD04) and the Chinese Scholarship Council (CSC). These sponsorships made the visiting appointments of Ma, Chen, and Wang at the USDA Forest Products Laboratory possible.

Author contributions: All the authors have accepted responsibility for the entire content of this submitted manuscript and approved submission.

Employment or leadership: None declared.
Honorarium: None declared.

References

Ago, M., Huan, S., Borghei, M., Raula, J., Kauppinen, E.I., Rojas, O.J. (2016) High-throughput synthesis of lignin particles (~30 nm to ~2 μm) via aerosol flow reactor: size fractionation and utilization in pickering emulsions. ACS Appl. Mater. Interfaces 8:23302–23310.

Bian, H., Chen, L., Gleisner, R., Dai, H., Zhu, J.Y. (2017) Producing wood-based nanomaterials by rapid fractionation of wood at 80°C using a recyclable acid hydrotrope. Green Chem. 19:3370–3379.

Chen, L., Dou, J., Ma, Q., Li, N., Wu, R., Bian, H., Yelle, D.J., Vuorinen, T., Fu, S., Pan, X., Zhu, J.Y. (2017) Rapid and near-complete dissolution of wood lignin at ≤80°C by a recyclable acid hydrotrope. Sci. Adv. 3:e1701735.

Cheng, G., Kent, M.S., He, L., Varanasi, P., Dibble, D., Arora, R., Deng, K., Hong, K., Melnichenko, Y.B., Simmons, B.A., Singh, S. (2012) Effect of ionic liquid treatment on the structures of lignins in solutions: molecular subunits released from lignin. Langmuir 28:11850–11857.

Frangville, C., Rutkevičius, M., Richter, A.P., Velev, O.D., Stoyanov, S.D., Paunov, V.N. (2012) Fabrication of environmentally biodegradable lignin nanoparticles. ChemPhysChem 13:4235–4243.

Ji, H., Chen, L., Zhu, J.Y., Gleisner, R., Zhang, X. (2016) Reaction kinetics based optimization of furfural production from corncob using a fully recyclable solid acid. Ind. Eng. Chem. Res. 55:11253–11259.

Jiang, C., He, H., Jiang, H., Ma, L., Jia, D. (2013) Nano-lignin filled natural rubber composites: preparation and characterization. Express Polym. Lett. 7:480–493.

Kumari, A., Yadav, S.K., Yadav, S.C. (2010) Biodegradable polymeric nanoparticles based drug delivery systems. Colloids Surf. B Biointerfaces 75:1–18.

Kunz, W., Holmberg, K., Zemb, T. (2016) Hydrotropes. Curr. Opin. Colloid Interface Sci. 22:99–107.

Lazarus, W., Headlee, W.L., Zalesny, R.S. (2015) Impacts of supply-shed-level differences in productivity and land costs on the economics of hybrid poplar production in Minnesota, USA William Lazarus. BioEnergy Res. 8:231–248.

Li, C., Zhao, X., Wang, A., Huber, G.W., Zhang, T. (2015) Catalytic transformation of lignin for the production of chemicals and fuels. Chem. Rev. 115:11559–11624.

Lievonen, M., Valle-Delgado, J.J., Mattinen, M.-L., Hult, E.-L., Lintinen, K., Kostiainen, M.A., Paananen, A., Szilvay, G.R., Setälä, H., Österberg, M. (2016) A simple process for lignin nanoparticle preparation. Green Chem. 18:1416–1422.

Lu, Q., Zhu, M., Zu, Y., Liu, W., Yang, L., Zhang, Y., Zhao, X., Zhang, X., Zhang, X., Li, W. (2012) Comparative antioxidant activity of nanoscale lignin prepared by a supercritical antisolvent (SAS) process with non-nanoscale lignin. Food Chem. 135:63–67.

Myint, A.A., Lee, H.W., Seo, B., Son, W.-S., Yoon, J., Yoon, T.J., Park, H.J., Yu, J., Yoon, J., Lee, Y.-W. (2016) One pot synthesis of environmentally friendly lignin nanoparticles with compressed

liquid carbon dioxide as an antisolvent. Green Chem. 18: 2129–2146.

Nair, S.S., Sharma, S., Pu, Y., Sun, Q., Pan, S., Zhu, J.Y., Deng, Y., Ragauskas, A.J. (2014) High shear homogenization of lignin to nanolignin and thermal stability of nanolignin-polyvinyl alcohol blends. ChemSusChem 7:3513–3520.

Popa, V.I., Căpraru, A.M., Grama, S., Măluţan, T. (2011) Nanoparticles based on modified lignins with biocide properties. Cell. Chem. Technol. 45:221–226.

Procter, A.R. (1971) A review of hydrotropic pulping. Pulp Pap. Mag. Can. 72:67–74.

Qian, Y., Zhang, Q., Qiu, X., Zhu, S. (2014) CO_2-responsive diethylaminoethyl-modified lignin nanoparticles and their application as surfactants for CO_2/N_2-switchable Pickering emulsions. Green Chem. 16:4963–4968.

Ragauskas, A.J., Beckham, G.T., Biddy, M.J., Chandra, R., Chen, F., Davis, M.F., Davison, B.H., Dixon, R.A., Gilna, P., Keller, M., Langan, P., Naskar, A.K., Saddler, J.N., Tschaplinski, T.J., Tuskan, G.A., Wyman, C.E. (2014) Lignin valorization: improving lignin processing in the biorefinery. Science 344:1246843.

Richter, A.P., Brown, J.S., Bharti, B., Wang, A., Gangwal, S., Houck, K., Cohen Hubal, E.A., Paunov, V.N., Stoyanov, S.D., Velev, O.D. (2015) An environmentally benign antimicrobial nanoparticle based on a silver-infused lignin core. Nat. Nanotechnol. 10:817–823.

Richter, A.P., Bharti, B., Armstrong, H.B., Brown, J.S., Plemmons, D., Paunov, V.N., Stoyanov, S.D., Velev, O.D. (2016) Synthesis and characterization of biodegradable lignin nanoparticles with tunable surface properties. Langmuir 32:6468–6477.

Shikinaka, K., Fujii, N., Egashira, S., Murakami, Y., Nakamura, M., Otsuka, Y., Ohara, S., Shigehara, K. (2010) Polyfunctional nanometric particles obtained from lignin, a woody biomass resource. Green Chem. 12:1914–1916.

Shimizu, S., Matubayasi, N. (2014) Hydrotropy: monomer-micelle equilibrium and minimum hydrotrope concentration. J. Phys. Chem. B 118:10515–10524.

Shuai, L., Amiri, M.T., Questell-Santiago, Y.M., Héroguel, F., Li, Y., Kim, H., Meilan, R., Chapple, C., Ralph, J., Luterbacher, J.S. (2016) Formaldehyde stabilization facilitates lignin monomer production during biomass depolymerization. Science 354:329–333.

Tortora, M., Cavalieri, F., Mosesso, P., Ciaffardini, F., Melone, F., Crestini, C. (2014) Ultrasound driven assembly of lignin into microcapsules for storage and delivery of hydrophobic molecules. Biomacromolecules 15:1634–1643.

Tupciauskas, R., Gravitis, J., Abolins, J., Veveris, A., Andzs, M., Liitia, T., Tamminen, T. (2017) Utilization of lignin powder for manufacturing self-binding HDF. Holzforschung 71:555–561.

Wang, Y.Y., Chen, Y.R., Sarkanen, S. (2015) Path to plastics composed of ligninsulphonates (lignosulfonates). Green Chem. 17:5069–5078.